

Nonclassicality of photon-modulated atomic coherent states in the Schwinger bosonic realization

Jisuo Wang(王继锁)[1,†], Xiangguo Meng(孟祥国)[2,‡], and Xiaoyan Zhang(张晓燕)[1,2]

Citation: Chin. Phys. B, 2020, 29 (**12**): 124213. DOI: 10.1088/1674-1056/abb3e8
Journal homepage: http://cpb.iphy.ac.cn; http://iopscience.iop.org/cpb

What follows is a list of articles you may be interested in

Finite-dimensional pair coherent state engendered via the nonlinear Bose operator realization and its Wigner phase-space distributions

Jianming Liu(刘建明), Xiangguo Meng(孟祥国)
Chin. Phys. B, 2019, 28 (**12**): 124206. DOI: 10.1088/1674-1056/ab4f5f

Higher-order nonclassical effects generated by multiple-photon annihilation-then -creation and creation-then-annihilation coherent states

Hong-Chun Yuan(袁洪春), Xue-Xiang Xu(徐学翔), Jin Xiao(肖进), Chao Xiong(熊超), Xi-Fang Zhu(朱锡芳)
Chin. Phys. B, 2016, 25 (**5**): 054202. DOI: 10.1088/1674-1056/25/5/054202

Algebraic and group treatments to nonlinear displaced number statesand their nonclassicality features: A new approach

N Asili Firouzabadi, M K Tavassoly, M J Faghihi
Chin. Phys. B, 2015, 24 (**6**): 064204. DOI: 10.1088/1674-1056/24/6/064204

Wigner function and the entanglement of quantized Bessel–Gaussian vortex state of quantized radiation field

Zhu Kai-Cheng, Li Shao-Xin, Tang Ying, Zheng Xiao-Juan, Tang Hui-Qin
Chin. Phys. B, 2012, 21 (**8**): 084204. DOI: 10.1088/1674-1056/21/8/084204

Nonclassicality of a two-variable Hermite polynomial state

Tan Guo-Bin,Xu Li-Juan,Ma Shan-Jun
Chin. Phys. B, 2012, 21 (**4**): 044210. DOI: 10.1088/1674-1056/21/4/044210

Nonclassicality of photon-modulated atomic coherent states in the Schwinger bosonic realization*

Jisuo Wang(王继锁)[1,†], Xiangguo Meng(孟祥国)[2,‡], and Xiaoyan Zhang(张晓燕)[1,2]

[1] *Shandong Provincial Key Laboratory of Laser Polarization and Information Technology, College of Physics and Engineering, Qufu Normal University, Qufu 273165, China*

[2] *Shandong Provincial Key Laboratory of Optical Communication Science and Technology, School of Physical Science and Information Engineering, Liaocheng University, Liaocheng 252059, China*

(Received 3 July 2020; accepted manuscript online 1 September 2020)

We theoretically introduce two new photon-modulated atomic coherent states (ACSs) via using the Schwinger bosonic representation of the angular momentum operators (the sequential operations $J_{\pm}^{n}$) on an ACS, and investigate their nonclassicality using the Wigner distribution, photon number distribution, and entanglement entropy. It is found that photon-modulated ACSs possess more stronger nonclassicality than the original ACS in certain regions of τ, the nonclassicality enhances with increasing number n of the operations $J_{\pm}$ and the operation $J_{+(-)}^{n}$ enhances the entanglement in the region of small (large) τ.

Keywords: photon-modulated atomic coherent state, nonclassicality, Wigner distribution, entanglement

PACS: 42.50.−p, 03.65.−w, 05.30.−d **DOI:** 10.1088/1674-1056/abb3e8

1. Introduction

Non-Gaussian entangled states can frequently be used as a new class of physical carriers in quantum computation and quantum information. This is principally because such states can compensate for the shortcomings of traditional Gaussian states in quantum information processing, for instances, completing universal quantum computation and realizing the best entanglement distillation that determines the success or failure of quantum communication.

Among all the non-Gaussian entangled states, atomic coherent state (ACS) is widely used in various fields of quantum physics since it exhibits some remarkable nonclassicality and entanglement. Using the ACS, light scattering from an atomic system under cooperative conditions is examined,[1] and the interference pattern with steady relative phase in the interference between two Bose–Einstein condensates is analytically calculated.[2] In terms of the entangled state representation of ACS, the ACS can be viewed as the energy eigenstates of the anisotropic harmonic oscillator in a uniform magnetic field,[3] and we prove that the ACS keeps its form-invariant with time evolution when it is governed by a particular Hamiltonian.[4] Experimentally, the ACSs can be generated using many methods, for instance, using cavity QED and trapped ions.[5] Besides, the ACSs can be used to construct some generalized quantum states with spin squeezing and entanglement, such as excited ACSs,[6] superpositions of ACSs,[7] and hole-burning in ACSs,[8] etc.

Photon addition, photon subtraction, and their coherent superpositions are considered as a class of effective methods for preparing the non-Gaussian entangled states,[9–14] which is because these operations lead to some remarkable physical properties such as non-Gaussian, nonclassicality, and entanglement that completely differ from the initial Gaussian states. For example, photon addition and photon subtraction can enhance the entanglement of a two-mode squeezed state.[15,16] Reference [5] pointed out that the spin squeezing behavior of the so-called spin squeezing states is generated in some certain ranges of the relevant parameters via performing the ladder operations on an ACS. Enlightened by this, in this paper, we introduce two new photon-modulated ACSs in the Schwinger bosonic realization and investigate how the sequential operations can enhance the nonclassicality of the original ACS in terms of the Wigner distribution (WD), photon number distribution, and entangled entropy.

This paper is organized as follows. In Section 2, the WD for the ACS and its negative volume are discussed analytically and numerically. In Section 3, two new photon-modulated ACSs are theoretically constructed via the Schwinger bosonic representation of the angular momentum operators. Section 4 is devoted to investigating the WDs for the new photon-modulated ACSs and showing how the sequential operations enhance the nonclassicality of the original ACS in terms of the partial negativity of the WDs. In Section 5, the photon number distributions and Neumann entropy (entanglement) of the photon-modulated ACSs are investigated. Several main results are presented in Section 6.

*Project supported by the National Natural Science Foundation of China (Grant No. 11347026) and the Natural Science Foundation of Shandong Province, China (Grant Nos. ZR2016AM03 and ZR2017MA011).

†Corresponding author. E-mail: jswang@qfnu.edu.cn

‡Corresponding author. E-mail: mengxiangguo1978@sina.com

© 2020 Chinese Physical Society and IOP Publishing Ltd

2. Atomic coherent state and its Wigner distribution

The Schwinger bosonic representation of the angular momentum operators is

$$J_+ = a^\dagger b,\ \ J_- = ab^\dagger,\quad J_z = \frac{a^\dagger a - b^\dagger b}{2}, \tag{1}$$

which yield the following SU(2) Lie algebra:

$$[J_+, J_-] = 2J_z,\ \ [J_z, J_\pm] = \pm J_\pm, \tag{2}$$

where $a^\dagger$ and $b^\dagger$ are the bosonic creation operators of two-mode light fields. So the ACS in the Schwinger bosonic realization is expressed as[17,18]

$$\begin{aligned}|\tau\rangle &= \exp(\mu J_+ - \mu^* J_-)|0, 2j\rangle \\ &= (1+|\tau|^2)^{-j}\sum_{l=0}^{2j}\left(\begin{array}{c}2j\\ l\end{array}\right)^{1/2}\tau^l|l, 2j-l\rangle,\end{aligned} \tag{3}$$

where $\mu = \theta\,\mathrm{e}^{-\mathrm{i}\varphi}/2$ and $\tau = \mathrm{e}^{-\mathrm{i}\varphi}\tan(\theta/2)$. It then follows that the set of the ACSs can form a completeness quantum mechanics space since there is the relation

$$\sum_{j=0,1/2,1,3/2,\ldots}^{\infty}(2j+1)\int\frac{\sin\theta\,\mathrm{d}\theta\,\mathrm{d}\phi}{4\pi}|\tau\rangle\langle\tau| = 1. \tag{4}$$

Using the coherent state representation of the two-mode Wigner operator, namely, $\Delta(\alpha,\beta)$, we obtain the WD of two-mode Fock state $|l, 2j-l\rangle$ as

$$\begin{aligned}\mathcal{W} &= \frac{1}{\pi^2 l!(2j-l)!}H_{l,l}(2\alpha, 2\alpha^*) \\ &\quad\times H_{2j-l,2j-l}(2\beta, 2\beta^*)\,\mathrm{e}^{-2(|\alpha|^2+|\beta|^2)},\end{aligned} \tag{5}$$

which is proportional to the product of two two-variable Hermite polynomials of different orders, i.e., $H_{l,l}(2\alpha, 2\alpha^*)H_{2j-l,2j-l}(2\beta, 2\beta^*)$, namely, no entanglement and squeezing in the state $|l, 2j-l\rangle$. By combining Eqs. (3) and (5), and using the generalized binomial theorem involving two-variable Hermite polynomials[19]

$$\begin{aligned}&\sum_{l=0}^{m}\sum_{k=0}^{n}\left(\begin{array}{c}m\\ l\end{array}\right)\left(\begin{array}{c}n\\ k\end{array}\right)f^l g^k H_{l,k}(\mu,\nu)H_{m-l,n-k}(x,y) \\ &= \left(\sqrt{1+fg}\right)^{m+n}H_{m,n}\left(\frac{f\mu+x}{\sqrt{1+fg}}, \frac{g\nu+y}{\sqrt{1+fg}}\right),\end{aligned} \tag{6}$$

the WD for the ACS is obtained as

$$W_{\mathrm{ACS}} = \frac{(-1)^{2j}}{\pi^2}L_{2j}\left(\frac{4|\tau\alpha+\beta|^2}{1+|\tau|^2}\right)\mathrm{e}^{-2(|\alpha|^2+|\beta|^2)}, \tag{7}$$

where the relation $(-1)^n n! L_n(|\alpha|^2) = H_{n,n}(\alpha,\alpha^*)$ is used, $L_n(\cdot)$ is the Laguerre polynomial.[20] This indicates that the WD for the ACS in the Schwinger bosonic representation just corresponds to a Laguerre polynomial. Hence, we conclude that the ACS is said to be an entangled state due to the cross term between the variables α and β in $L_{2j}(\cdot)$, and the exponential term $(-1)^{2j}$ causes the ACS to be non-Gaussian. Indeed, the EPR entangled state $|\eta\rangle$ representation of two-mode Wigner operator $\Delta(\alpha,\beta)$ is expressed as[21,22]

$$\Delta(\rho,\varkappa) = \int\frac{\mathrm{d}^2\eta}{\pi^3}|\rho-\eta\rangle\langle\rho+\eta|\exp(\eta\varkappa^* - \eta^*\varkappa), \tag{8}$$

where the distribution W_{ACS} can also be obtained after a rigorous calculation, $\rho, \varkappa$ are complex, and the EPR entangled state $|\eta\rangle = \mathrm{e}^{-|\eta|^2/2+\eta a^\dagger - \eta^* b^\dagger + a^\dagger b^\dagger}|00\rangle$ ($\eta = \eta_1 + \mathrm{i}\eta_2$) is the common eigenstate of two particles' relative position $Q_1 - Q_2$ and the total momentum $P_1 + P_2$ in two-mode Fock space. When taking $\rho = \alpha + \beta^*$ and $\gamma = \alpha - \beta^*$, we can write $\Delta(\rho,\gamma)$ as two-mode Wigner operators $\Delta(\alpha,\beta)$ in the coherent state representation.

In Fig. 1, we plot the WD for the ACS as a function of $\mathrm{Re}\beta$ ($\mathrm{Im}\beta = \alpha = 0$) for different parameter values of j and τ. From Figs. 1(a) and 1(b), we clearly see that the WD always shows an upward major peak for a natural number j but a downward major peak for a semi-integer j at the central position of the phase space. With increasing natural number (or semi-integer) j, the position and the value of the major peak remain unchanged but its peak width gradually narrows. Also, the downward minor peaks gradually move closer to the center of the phase space and its numbers significantly increase since the total number is always two-mode photon number sum $2j$ of the ACS. Intuitively, it seems that the negative volume of the WF for a semi-integer j always larger than that for a natural number j as a result of the downward major peak for semi-integer j, which shows that the nonclassicality of the ACS for a semi-integer j can be more stronger than that for a natural number j.

On the other hand, for a given value of j (e.g., $j = 3$ or 3.5), the peak value and the position of the major peak remain unchanged and the major peak width widens as τ increases. However, the minor peaks move away from the center of the phase space and its numbers and peak values gradually decrease. For a certain threshold value of τ, all the minor peaks completely disappear and only the downward major peak is preserved for a semi-integer j. However, for a natural number j, the WD for the ACS always has two downward minor peaks adjacent to the upward major peak in the phase space, even for a large enough value of τ. This shows that the increase of the parameter τ can decrease the nonclassicality of the ACS but cannot completely lead to the disappearance of its nonclassicality.

Further, in order to clearly see how the parameters τ and j affect the nonclassicality of the ACS, we here quantify the negative volume of the WD $w(p,q)$ that is represented as the integral $V = \frac{1}{2}\int\mathrm{d}q\,\mathrm{d}p[|w(p,q)| - w(p,q)]$.[23,24] Substituting Eq. (7) into this integral formula, we numerically plot the negative volumes with the parameters τ and j in Fig. 1(c). Clearly, the negative volume for semi-integer j is generally larger than that for natural number j. The negative volume increases at

the initial stage of τ and then decreases at the remaining stages with natural number j, but it always decreases in the whole region of τ with semi-integer j. Hence, when the semi-integer j is large enough, the negative volume with a semi-integer j may be smaller than that with a natural number j. Besides, for a given j, the negative volume always decreases monotonically as τ increases. In summary, the ACS for semi-integer j has usually much stronger nonclassicality than that for natural number j, and the nonclassicality of the ACS gradually decreases with the parameter τ.

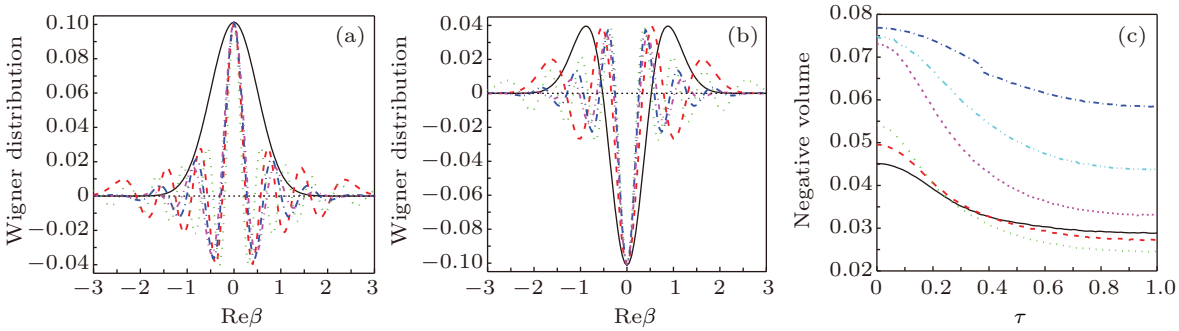


Fig. 1. Wigner distribution $W_{\rm ACS}$ for the ACS as a function of Reβ (Im$\beta=\alpha=0$) at (a) $\tau=0.3$ and $q=0$ (black solid), 3 (red dashed), 5 (green dotted); $j=3$ and $\tau=0.6$ (blue dash-dotted), 0.8 (magenta dash-dot-dotted); (b) $\tau=0.3$ and $j=0.5$ (black solid), 1.5 (red dashed), 3.5 (green dotted); $j=3.5$ and $\tau=0.6$ (blue dash-dotted), 0.8 (magenta dash-dot-dotted); (c) the negative volume of the distribution $W_{\rm ACS}$ as a function of τ for $j=2$ (black solid), 3 (red dashed), 5 (green dotted), 0.5 (blue dash-dotted), 1.5 (cyan dash-dot-dotted), 3.5 (magenta short-dashed).

3. Photon-modulated ACS

Motivated by the significant work of Gerry and coworkers that investigates the effect of the angular momentum ladder operations on the ACS, in this section we introduce two new photon-modulated ACSs via repeatedly performing the sequential operations $J_\pm$ on the initial ACS, which are specifically expressed as

$$\begin{aligned}|\tau;J_+,n\rangle &= \mathcal{N}_+^{1/2}(J_+)^n|\tau\rangle \\ &= \frac{\mathcal{N}_+^{1/2}}{(1+|\tau|^2)^j}\sum_{l=n}^{2j}\binom{2j}{l}^{1/2}\frac{l!\tau^{l-n}}{(l-n)!}|l,2j-l\rangle, \end{aligned} \tag{9}$$

$$\begin{aligned}|\tau;J_-,n\rangle &= \mathcal{N}_-^{1/2}(J_-)^n|\tau\rangle \\ &= \frac{\mathcal{N}_-^{1/2}}{(1+|\tau|^2)^j}\sum_{l=0}^{2j-n}\binom{2j}{l}^{1/2}\frac{(2j-l)!\tau^{l+n}}{(2j-l-n)!}|l,2j-l\rangle, \end{aligned} \tag{10}$$

where the normalized factors $N_\pm$ are

$$\begin{aligned}\mathcal{N}_+ &= \left[\sum_{l=n}^{2j}\frac{(2j)!l!|\tau|^{2(l-n)}}{(2j-l)![(l-n)!]^2(1+|\tau|^2)^{2j}}\right]^{-1}, \\ \mathcal{N}_- &= \left[\sum_{l=0}^{2j-n}\frac{(2j)!(2j-l)!|\tau|^{2(l+n)}}{l![(2j-l-n)!]^2(1+|\tau|^2)^{2j}}\right]^{-1}. \end{aligned} \tag{11}$$

Specially, assuming $\tau\ll 1$ and $n=1$, $j=1$, thus the states $|\tau;J_\pm,n\rangle$ become the superpositions of several special Fock states, which can be physically realized, i.e.,

$$\begin{aligned}J_+|\tau\rangle &\approx |1,1\rangle+\mathrm{e}^{-\mathrm{i}\varphi}|2,0\rangle, \\ J_-|\tau\rangle &\approx \mathrm{e}^{-\mathrm{i}2\varphi}|1,1\rangle+\mathrm{e}^{-\mathrm{i}\varphi}|0,2\rangle, \end{aligned} \tag{12}$$

which easily leads to

$$\begin{aligned}&tJ_++rJ_-|\tau\rangle \\ &\approx (t+r\mathrm{e}^{-\mathrm{i}2\varphi})|1,1\rangle+t\mathrm{e}^{-\mathrm{i}\varphi}|2,0\rangle+r\mathrm{e}^{-\mathrm{i}\varphi}|0,2\rangle, \end{aligned} \tag{13}$$

where t and r are respectively the real ratios of the operations J_+ and J_-. Furthermore, for the case of $n=1$ and $j=3/2$, we similarly have

$$\begin{aligned}J_+|\tau\rangle &\approx |1,2\rangle+\mathrm{e}^{-\mathrm{i}\varphi}|2,1\rangle+\mathrm{e}^{-\mathrm{i}2\varphi}|3,0\rangle, \\ J_-|\tau\rangle &\approx \mathrm{e}^{-\mathrm{i}\varphi}|0,3\rangle+\mathrm{e}^{-\mathrm{i}2\varphi}|1,2\rangle+\mathrm{e}^{-\mathrm{i}3\varphi}|2,1\rangle. \end{aligned} \tag{14}$$

It then follows

$$\begin{aligned}tJ_++rJ_-|\tau\rangle \approx{}& \left(t+r\mathrm{e}^{-\mathrm{i}2\varphi}\right)|1,2\rangle+t\mathrm{e}^{-\mathrm{i}2\varphi}|3,0\rangle \\ &+\mathrm{e}^{-\mathrm{i}\varphi}\left(t+r\mathrm{e}^{-\mathrm{i}2\varphi}\right)|2,1\rangle+r\mathrm{e}^{-\mathrm{i}\varphi}|0,3\rangle. \end{aligned} \tag{15}$$

4. Wigner distribution

Similar to obtaining the WD of the ACS, using the WD $\mathcal{W}$ of the state $|l,2j-l\rangle$ in Eqs. (5) and (9)–(11), the WDs of the states $|\tau;J_\pm,n\rangle$ are respectively given as

$$\mathcal{W}_+=\sum_{l=n}^{2j}d_+^2\mathcal{W},\quad \mathcal{W}_-=\sum_{l=0}^{2j-n}d_-^2\mathcal{W}, \tag{16}$$

where

$$\begin{aligned}d_+^2 &= \mathcal{N}_+\frac{l!(2j)!|\tau|^{2(l-n)}}{(2j-l)![(l-n)!]^2(1+|\tau|^2)^{2j}}, \\ d_-^2 &= \mathcal{N}_-\frac{(2j)!(2j-l)!|\tau|^{2(l+n)}}{l![(2j-l-n)!]^2(1+|\tau|^2)^{2j}}. \end{aligned} \tag{17}$$

Noting that the distribution $\mathcal{W}$ cannot show any entanglement and squeezing in terms of the natural characters of Fock states, thus we say that the entanglement and squeezing of the states $|\tau;J_\pm,n\rangle$ completely come from the superposition of the distribution $\mathcal{W}$.

In Fig. 2, we plot the WD of the state $|\tau;J_+,n\rangle$ as a function of Reβ (Im$\beta=\alpha=0$) for $\tau=0.3$ and different values

of j and n. Figures 2(a) and 2(b) show that, for any parameter value of j,τ, or n, the peak value and the position of the upward major peak remain unchanged, which is similar to the result of the WD for the original ACS. Compared with the original ACS, the peak width of the major peak widens and the number and the peak values of the minor peaks decrease as the number n of the operation J_+ is increased. Specially, when $n=2j$, the distributions $\mathcal{W}_+$ lose all the minor peaks and only show the major peak. This major peak cannot change with the parameter τ since the terms on τ disappear in the analytical result (16).

Figure 2(c) shows that the negative volume of the distribution $\mathcal{W}_+$ is always much larger than that of the original ACS in the whole region of τ for a natural number j or in the region of large τ for a semi-integer j, and gradually increases with increasing n in the region of large τ for a fixed value of j. So, we conclude that the state $|\tau;J_+,n\rangle$ has much stronger nonclassicality than the original ACS for all τ when j is a natural number or for large τ when j is a semi-integer, and the nonclassicality can be enhanced with increasing n for large τ.

Figure 3 presents the WD of the state $|\tau;J_-,n\rangle$ of Reβ (Im$\beta=\alpha=0$) for different parameter values of j and n. Obviously, the major peaks of the distributions $\mathcal{W}_-$ are almost coincident for any value of j,τ, and n, but the peak values of the minor peaks far from the major peak significantly increase with increasing n for any j. The distribution $\mathcal{W}_-$ of the state $|\tau;J_-,n\rangle$ has much larger negative volume than that of the original ACS for all τ (except for $\tau=0$) and a fixed j, and the negative volume increases with increasing number n of the operation J_-. This result shows that the state $|\tau;J_-,n\rangle$ exhibits much stronger nonclassicality than the original ACS in the whole region of τ for all j and the nonclassicality can be enhanced with the increase of n.

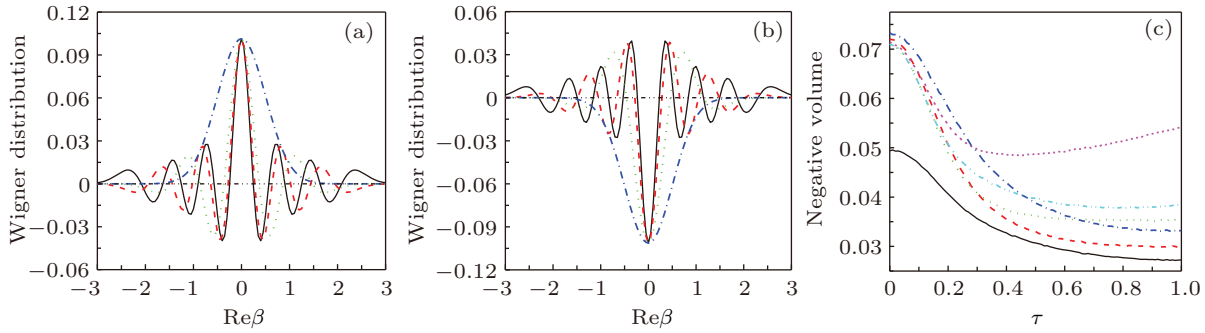


Fig. 2. Wigner distribution $\mathcal{W}_+$ for the photon-modulated ACS $|\tau;J_+,n\rangle$ of Reβ (Im$\beta=\alpha=0$) for $\tau=0.3$ and its negative volume. (a) $j=3$ with $n=0$ (black solid), 1 (red dashed), 3 (green dotted), and 6 (blue dash-dotted), (b) $j=3.5$ with $n=0$ (black solid), 2 (red dashed), 5 (green dotted), and 7 (blue dash-dotted), (c) the negative volume of the distribution $\mathcal{W}_+$ for $j=3$ with $n=0$ (black solid), 1 (red dashed), 3 (green dotted); $j=3.5$ and $n=0$ (blue dash-dotted line), 2 (cyan dash-dotted-dotted), and 5 (magenta short-dashed).

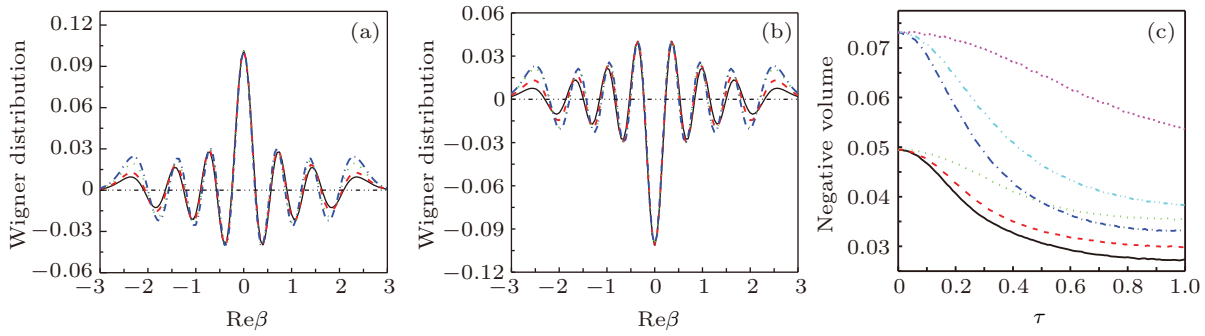


Fig. 3. Wigner distribution for the photon-modulated ACS $|\tau;J_-,n\rangle$ of Reβ (Im$\beta=\alpha=0$) in (a) and (b) and its negative volume in (c) for different parameter values of τ, j, and n, where the values of τ, j, and n are the same as those in Fig. 2.

5. Photon number distribution and entanglement entropy

For the photon-modulated ACSs $|\tau;J_\pm,n\rangle$, the photon number distributions $|\langle m_a,m_b|\tau;J_\pm,n\rangle|^2$ refer to the probabilities of finding (m_a,m_b) photons in the light fields,[25,26] which is usually used as an important quantum statistical property. Thus, we give the photon number distributions of the states $|\tau;J_\pm,n\rangle$ respectively as

$$P_+(m_a,m_b) = \frac{\mathcal{N}_+(2j)!m_a!\,|\tau|^{2(m_a-n)}\,\delta_{m_b,2j-m_a}}{(1+|\tau|^2)^{2j}(2j-m_a)!\,[(m_a-n)!]^2},$$
$$P_-(m_a,m_b) = \frac{\mathcal{N}_-(2j)!(2j-m_a)!\,|\tau|^{2(m_a+n)}\,\delta_{m_b,2j-m_a}}{(1+|\tau|^2)^{2j}m_a!\,[(2j-m_a-n)!]^2}, \quad (18)$$

which show that the photon number distributions $P_\pm(m_a,m_b)$ are governed by the restraint condition $m_b=2j-m_a$. Specifically, the probabilities of finding only several (m_a,m_b)

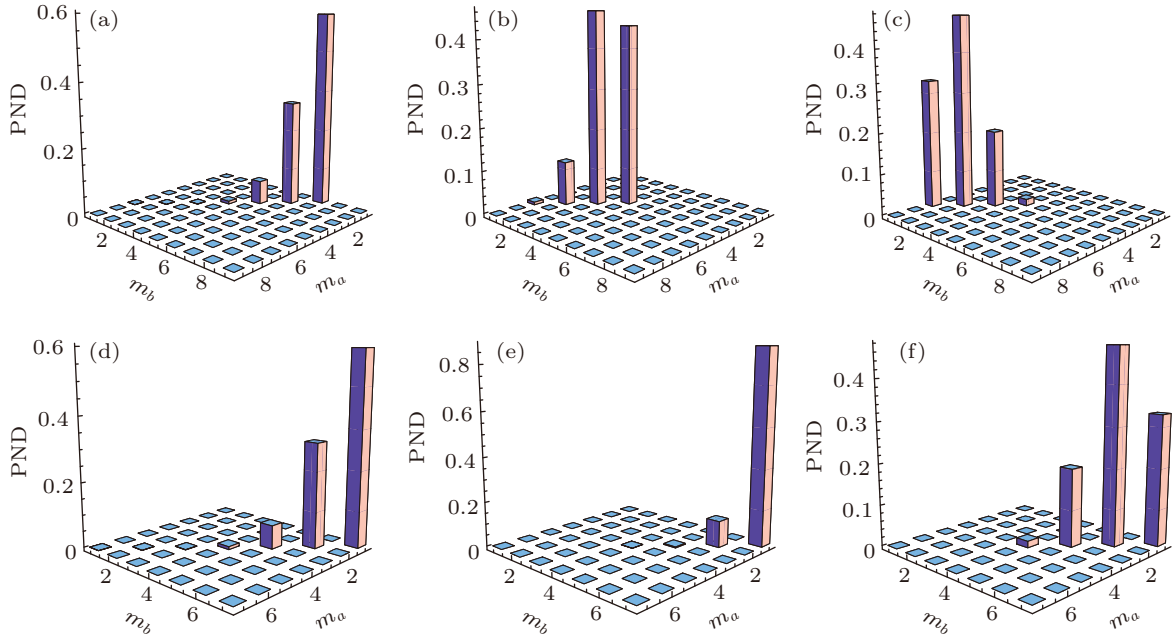


Fig. 4. Photon number distributions (PNDs) $P_{\pm}(m_a,m_b)$ of photon-modulated ACSs $|\tau;J_{\pm},n\rangle$ in the two-mode Fock space (m_a,m_b) for $j=3$ and different values of (τ,n): (a), (d) $(0.3,0)$; (b), (e) $(0.3,3)$; and (c), (f) $(1,3)$.

numbers of photons in the states $|\tau;J_{\pm},n\rangle$ cannot be zero as a result of the restraint condition $m_a+m_b=2j$, but the photon number distribution is always zero for $m_b\neq 2j-m_a$. It seems reasonable because the sum of photon numbers of two modes for the states $|\tau;J_{\pm},n\rangle$ is always $2j$.

Figure 4 shows the photon number distributions $P_{\pm}(m_a,m_b)$ of the states $|\tau;J_{\pm},n\rangle$ in (m_a,m_b) for different n and τ when $j=3$. Clearly, the photon number distribution only appears in several (m_a,m_b) photon numbers and is zero for others because of the restraint condition $m_a+m_b=2j$ in the analytical result (18). Compared with the original ACS, the operation J_+ can lead to the fact that photons appear in many more Fock states, but the role of J_+ is opposite. With increasing τ, more photons appear in Fock states and the peak value of the photon number distribution moves diagonally toward the smaller m_b photon numbers. And, as noted, the above results apply to all values of j.

For a two-mode entangled pure state $|\Phi\rangle_{ab}$, if there is the Schmidt decomposition

$$|\Phi\rangle_{ab}=\sum_{n=1} d_n|\alpha_n\rangle_a|\beta_n\rangle_b$$

with the mutually orthonormal states $|\alpha_n\rangle_a,|\beta_n\rangle_b$, and the real positive coefficient d_n, then the entanglement of this state can be quantified using the partial Neumann entropy[27,28]

$$\mathcal{E}(|\Phi\rangle_{ab})=-\sum_{n=1} d_n^2\log_2 d_n^2.$$

Using the Schmidt decomposition of the states $|\tau;J_{\pm},n\rangle$ in Eqs. (9)–(11), their Neumann entropy can be directly obtained as

$$\mathcal{E}_+=-\sum_{l=n}^{2j} d_+^2\log_2 d_+^2,\quad \mathcal{E}_-=-\sum_{l=0}^{2j-n} d_-^2\log_2 d_-^2. \tag{19}$$

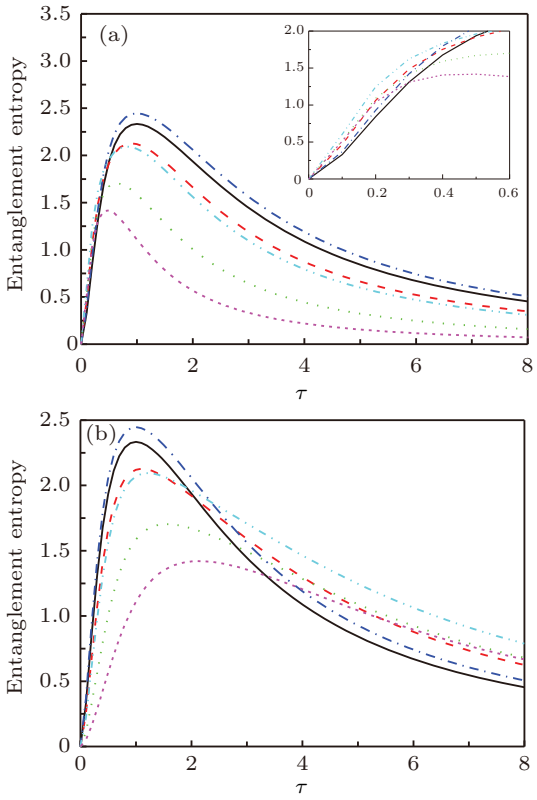


Fig. 5. (a), (b) Entanglement entropy of the photon-modulated ACSs (a) $|\tau;J_+,n\rangle$ and (b) $|\tau;J_-,n\rangle$ as a function of the parameter τ for $j=3$ with $n=0$ (black solid), 1 (red dashed), 3 (green dotted); $j=3.5$ and $n=0$ (blue dash-dotted), 2 (cyan dash-dot-dotted), and 5 (magenta short-dashed), respectively.

In Fig. 5, we plot the entanglement entropy of the states

$|\tau;J_{\pm},n\rangle$ as a function of τ for different parameter values of j and n. Figure 5 shows that, for any j, the entanglement of the states $|\tau;J_{\pm},n\rangle$ always increases rapidly and then decreases gradually with increasing τ, and always tends to zero when the value of τ is large enough. For any j, the state $|\tau;J_{+},n\rangle$ ($|\tau;J_{-},n\rangle$) has much stronger entanglement than the original ACS in the region of small (large) τ. Also, with increasing n, the entanglement of the states $|\tau;J_{\pm},n\rangle$ increases for a natural number j but decreases for a semi-integer j.

6. Conclusions

In summary, we have introduced two new photon-modulated ACSs via repeatedly acting the sequential operations $J_{\pm}$ on an ACS and discussed its WD, photon number distribution, and entanglement entropy. By analytical and numerical analysis, we have shown that, compared with the original ACS, the operations $J_{\pm}^{n}$ can enhance the nonclassicality in certain regions of τ, which gradually increases with increasing operation numbers n. Also, the entanglement of the photon-modulated ACSs can be enhanced by the operation $J_{+(-)}^{n}$ for small (large) τ. Besides, the photon number distribution is controlled by the condition $m_a + m_b = 2j$, that is, two-mode photon number sum $2j$ of the photon-modulated ACSs, and the operations $J_{\pm}$ have different effects on the photon number distributions of the original ACS.

References

[1] Agarwal G S, Feng D H, Narducci L M, Gilmore R and Tuft R A 1979 *Phys. Rev. A* **20** 2040
[2] Tang X B and Fan H Y 2008 *Commun. Theor. Phys.* **50** 1145
[3] Meng X G, Wang J S and Liang B L 2010 *Chin. Phys. B* **19** 124205
[4] Wang J S, Meng X G and Fan H Y 2019 *Chin. Phys. B* **28** 100301
[5] Gerry C G and Adil B 2008 *Phys. Rev. A* **77** 062341
[6] Obada A S F and Abd Al-kader G M 2002 *J. Mod. Opt.* **50** 2163
[7] Berrada K, Abdel Khalek S and Raymond Ooi C H 2012 *Phys. Rev. A* **86** 033823
[8] Gerry C G and Mark P 2008 *Phys. Lett. A* **372** 6480
[9] Kitagawa A, Takeoka M, Sasaki M and Chefles A 2006 *Phys. Rev. A* **73** 042310
[10] Meng X G, Li K C, Wang J S, Zhang X Y, Zhang Z T, Yang Z S and Liang B L 2020 *Ann. Phys.* **532** 1900585
[11] Meng X G, Wang Z, Fan H Y, Wang J S and Yang Z S 2012 *J. Opt. Soc. Am. B* **29** 1844
[12] Meng X G, Li K C, Wang J S, Yang Z S, Zhang X Y, Zhang Z T and Liang B L 2020 *Front. Phys.* **15** 52501
[13] Wang Z, Meng X G and Fan H Y 2013 *J. Phys. A: Math. Theor.* **46** 135305
[14] Li K C, Meng X G and Wang J S 2019 *Commun. Theor. Phys.* **71** 807
[15] Bartley T J, Crowley P J D, Datta A, Nunn J, Zhang L and Walmsley I 2013 *Phys. Rev. A* **87** 022313.
[16] Olivares S, Paris M G A and Bonifacio R 2003 *Phys. Rev. A* **67** 032314
[17] Fan H Y, Li C and Jiang Z H 2004 *Phys. Lett. A* **327** 416
[18] Wang J S, Meng X G and Liang B L 2010 *Chin. Phys. B* **19** 014207
[19] Meng X G, Liu J M, Wang J S and Fan H Y 2019 *Eur. Phys. J. D* **73** 32
[20] Liu J M and Meng X G 2019 *Chin. Phys. B* **28** 124206
[21] Fan H Y, Hu L Y and Fan Y 2006 *Ann. Phys.* **321** 480
[22] Meng X G, Wang Z, Wang J S and Fan H Y 2013 *J. Opt. Soc. Am. B* **30** 1614
[23] Kenfack A and Życzkowski K 2004 *J. Opt. B: Quantum Semiclass. Opt.* **6** 396
[24] Li K C, Meng X G and Wang J S 2019 *Int. J. Theor. Phys.* **58** 2521
[25] Meng X G, Wang J S, Liang B L and Han C X 2018 *Front. Phys.* **13** 130322
[26] Meng X G, Goan H S, Wang J S and Zhang R 2018 *Opt. Commun.* **411** 15
[27] Bennett C H, Bernstein H J, Popescu S and Schumacher B 1996 *Phys. Rev. A* **53** 2046
[28] Xu X X 2015 *Phys. Rev. A* **92** 012318